

NNT : \*\*\*

n°LAL : \*\*\*

Thèse de doctorat

# Search of the $0\nu\beta\beta$ decay with the SuperNEMO demonstrator

Thèse de doctorat de l'Université Paris-Saclay  
préparée à l'Université Paris Saclay au sein du Laboratoire Irène-Joliot Curie  
(anciennement Laboratoire de l'Accélérateur Linéaire)

École doctorale n°576 Particles, Hadrons, Energy, Nuclei, Instrumentation,  
Imaging, Cosmos et Simulation (PHENIICS)  
Spécialité de doctorat : Physique des particules

Thèse présentée et soutenue à Orsay, le \*\*\*, par

**CLOÉ GIRARD-CARILLO**

## Composition du Jury :

***	
***	Président
***	
***	
***	Rapporteur
***	
***	
***	Rapporteur
Christine Marquet CENBG - Bordeaux-Gradignan	Examineur
***	
***	Examineur
***	
***	Examineur
Laurent Simard LAL - Orsay	Directeur de thèse
Mathieu Bongrand LAL - Orsay	Co-directeur de thèse



---

# Contents

<b>Contents</b>	<b>3</b>
<b>Introduction</b>	<b>7</b>
<b>1 Phenomenology of particle physics</b>	<b>9</b>
1.1 The Standard Model of particle physics . . . . .	9
1.1.1 Bosons . . . . .	9
1.1.2 Fermions . . . . .	9
1.1.3 $2\nu\beta\beta$ decay . . . . .	9
1.1.4 Where the Standard Model ends . . . . .	9
1.2 Going beyond the Standard Model with neutrinos . . . . .	9
1.2.1 Neutrino flavors and oscillations . . . . .	9
1.2.2 Neutrino masses and nature . . . . .	9
1.2.3 Other searches beyond the Standard Model with neutrinos . . . . .	9
<b>2 <math>0\nu\beta\beta</math> experiment status</b>	<b>11</b>
2.1 Experimental design criteria . . . . .	11
2.1.1 Aspects of the nuclear matrix elements . . . . .	12
2.1.2 Quenching . . . . .	12
2.2 $0\nu\beta\beta$ direct search experiments . . . . .	12
2.2.1 Semiconductors . . . . .	12
2.2.2 Bolometers . . . . .	14
2.2.3 Time projection chambers . . . . .	14
2.2.4 Scintillators . . . . .	16
2.2.5 Tracking calorimeters . . . . .	16
<b>3 The SuperNemo demonstrator</b>	<b>18</b>
3.1 The SuperNemo demonstrator . . . . .	18
3.1.1 Comparison with Nemo3 experiment . . . . .	18
3.1.2 Experimental design . . . . .	18
3.1.3 Sources . . . . .	18
3.1.4 Tracker . . . . .	18
3.1.5 Calorimeter . . . . .	18

3.1.5.1	Scintillator . . . . .	18
3.1.5.2	Photomultiplier . . . . .	18
3.1.6	Calibration systems . . . . .	18
3.1.7	Control Monitoring system . . . . .	18
3.1.8	Electronics . . . . .	18
3.2	The background of SuperNEMO . . . . .	18
3.2.1	Internal background . . . . .	18
3.2.2	External background . . . . .	18
3.2.3	Background specifications . . . . .	18
3.2.4	Measured demonstrator background levels . . . . .	18
3.3	The SuperNemo software . . . . .	18
3.3.1	Simulation . . . . .	18
3.3.2	Reconstruction . . . . .	19
<b>4</b>	<b>Analysis tools</b>	<b>21</b>
4.0.1	Internal probability . . . . .	21
4.1	Simulations . . . . .	22
4.1.1	Modifications of simulation software . . . . .	22
4.1.2	Internal background simulations . . . . .	22
4.1.3	$0\nu\beta\beta$ simulations . . . . .	22
<b>5</b>	<b>Time difference</b>	<b>23</b>
5.1	Principle and goal . . . . .	23
5.1.1	Internal conversion . . . . .	23
5.2	Analysis . . . . .	24
5.2.1	Topological cuts . . . . .	24
5.2.2	Exponentially modified Gaussian . . . . .	24
5.2.3	Results . . . . .	24
5.3	Conclusion . . . . .	24
<b>6</b>	<b>Sensitivity of the SuperNEMO demonstrator to the <math>0\nu\beta\beta</math></b>	<b>27</b>
6.1	Signal and background simulations . . . . .	27
6.2	Optimisation of event selection . . . . .	29
6.3	Expected number of background events . . . . .	31
6.4	Demonstrator sensitivity . . . . .	31
6.4.1	avec B . . . . .	31
6.4.2	sans B . . . . .	31
6.4.3	Champ mappé . . . . .	31
6.5	HyperNEMO . . . . .	31
6.6	Other isotopes . . . . .	31
6.7	Conclusion . . . . .	31
<b>7</b>	<b>Detector commissioning</b>	<b>31</b>
7.1	Reflectometry analysis . . . . .	31
7.1.1	Goal of the reflectometry analysis . . . . .	31
7.1.2	Pulse timing: controlling cable lengths . . . . .	32
7.1.3	Signal attenuation . . . . .	37

7.1.4	Pulse shape analysis . . . . .	39
7.1.5	Comparison with $^{60}\text{Co}$ . . . . .	39
7.1.6	Conclusion . . . . .	39
7.2	Calibrating the electronic boards . . . . .	39
7.2.1	Principle . . . . .	39
7.2.2	Measuring the time offset of front end boards . . . . .	39
7.2.3	Results . . . . .	39
7.3	Energy calibration of optical modules . . . . .	39
7.4	Baseline studies . . . . .	39
7.5	Light Injection System . . . . .	39
<b>8</b>	<b>Characterisation of the calorimeter time resolution</b>	<b>41</b>
8.1	Interaction of particles in the SuperNEMO scintillators . . . . .	42
8.1.1	Interaction of electrons . . . . .	42
8.1.2	Interaction of photons . . . . .	42
8.2	Measurement of the time resolution with a $^{60}\text{Co}$ source . . . . .	43
8.2.1	Description of Cobalt 60 nucleus . . . . .	44
8.2.2	Time response of optical modules . . . . .	44
8.2.3	Final experimental design . . . . .	47
8.2.4	Signal events selection . . . . .	49
8.2.5	Background estimation . . . . .	51
8.2.6	Detector efficiency . . . . .	55
8.2.7	Determination of the individual timing resolution of each optical module . . . . .	56
8.2.8	Conclusion . . . . .	60
8.3	The Light Injection System . . . . .	60
8.3.1	Light injection system commissioning . . . . .	61
8.3.2	Time resolution of optical modules . . . . .	61
	<b>Conclusion</b>	<b>63</b>
	<b>Bibliography</b>	<b>65</b>



## Sensitivity of the SuperNEMO demonstrator to the $0\nu\beta\beta$

In this chapter, we present the SuperNEMO sensitivity to the  $0\nu\beta\beta$  decay half-life, and the corresponding effective neutrino masses, for several isotopes. The SuperNEMO final detector is expected to exclude  $0\nu\beta\beta$  half-lives up to  $1.2 \times 10^{26}$  y (90% CL) if  $0\nu\beta\beta$  decays through the mass mechanism, with a detector exposure of 500 kg.y [7]. The sensitivity is given as a limit, in case we do not observe the expected signal. In 2010 began the demonstrator installation at the Laboratoire Souterrain de Modane. With an exposure of 17.5 y, the demonstrator could set a limit on the  $0\nu\beta\beta$  process of  $5.35 \times 10^{24}$  y (90% CL) [8].

This study aims to explore the impact on the sensitivity of the presence of a magnetic field, and will participate in the final decision on the installation of the coil. In a context of investigating the demonstrator and final detector capabilities, different internal source contamination levels are explored. The topology of interest is the two electrons topology, and we use the  $2e$  energy sum to discriminate the signal from the background events. Thanks to SuperNEMO tracking capabilities, topological informations are exploited to improve the SuperNEMO sensitivity.

### 6.1 Signal and background simulations

A full simulation for the SuperNEMO demonstrator was performed, in order to determine the longest  $0\nu\beta\beta$  half-life that can be probed with SuperNEMO using the distribution of the sum of electron energies, in the case where the  $0\nu\beta\beta$  decay were not observed. In the Tab. 6.1 is summarised the expected number of signal and background events, both for the SuperNEMO demonstrator and final detector, and we present the size of Monte-Carlo simulations for each isotope.

#### The $0\nu\beta\beta$ signal

In the following, the assumed underlying mechanism for the  $0\nu\beta\beta$  decay is the mass mechanism (MM), as it is the most natural and widespread mechanism. The hypothetical  $0\nu\beta\beta$  signal would be detected as an excess of events in the region of interest, with respect to the predicted background contamination level. The

	Expected decays		Simulated decays
	Demonstrator	Final detector	
$0\nu\beta\beta$ ( $T_{1/2}^{0\nu} = 2.5 \cdot 10^{23}$ y)	$3.6 \cdot 10^2$	$1.0 \cdot 10^4$	$1.0 \cdot 10^7$
$2\nu\beta\beta$	$9.5 \cdot 10^5$	$2.7 \cdot 10^7$	$1.0 \cdot 10^7$
$^{208}\text{Tl}$	$5.5 \cdot 10^3$	$1.6 \cdot 10^5$	$1.0 \cdot 10^7$
$^{214}\text{Bi}$	$1.1 \cdot 10^3$	$3.1 \cdot 10^4$	$1.0 \cdot 10^7$
$^{222}\text{Rn}$	$1.8 \cdot 10^5$	$7.2 \cdot 10^6$	$1.0 \cdot 10^7$

Table 6.1: Expected and simulated decays for different processes, both for the demonstrator (17.5 kg.y) and for the final detector (500 kg.y), assuming target background activities are reached.

$10^7$   $0\nu\beta\beta$  Monte-Carlo events are generated using the DECAY0 software [9]. The simulations are normalised assuming a  $T_{1/2}^{0\nu} = 6.0 \cdot 10^{24}$  y half-life [citation].

### Inside detector backgrounds

In the region where a signal of neutrinoless  $\beta\beta$  decay is expected, the allowed  $2\nu\beta\beta$  decay stands as the dominant internal background type. Its contribution depends on the  $2\nu\beta\beta$  half-life and the energy resolution of the detector. The total energy brought by the two electrons is a continuum presenting a reduced number of events in the region of interest, due to electron energy losses before reaching the calorimeter (mainly inside the dense source material, as well as inside the wire chamber). To adress this, we simulated  $10^7$   $2\nu\beta\beta$  events with a total energy  $> 2$  MeV, in addition of the normal  $2\nu\beta\beta$  decays, and we normalised the total  $2\nu\beta\beta$  spectrum.

Trace quantities of naturally-occurring radioactive isotopes can occasionally produce two-electron events and thus can mimic  $\beta\beta$ -decay events. The largest contributions come from isotopes of decay chains of  $^{238}\text{U}$ ,  $^{232}\text{Th}$  and  $^{40}\text{K}$ , which disintegration occur inside the source foils, as well as inside the tracking volume. As described in Sec. 3.2.1, source foil contaminations by isotopes such as  $^{208}\text{Tl}$  or  $^{214}\text{Bi}$  constitute the principal internal backgrounds with the  $2\nu\beta\beta$  decay. These backgrounds are processed by the same detector simulation as the  $0\nu\beta\beta$  signal, using DECAY0. Since internal backgrounds have very low efficiencies in the  $2e$  topology, we simulated an important amount of Monte-Carlo events.

A component of the external background producing events similar to the internal background is caused by the presence of  $^{222}\text{Rn}$  inside the tracking detector volume, and constitute a separate background category. If such a decay occurs on or near a foil and appears with a  $2e$  topology, it becomes hard to distinguish from a double beta decay candidate. This isotope being distributed throughout the whole tracking detection volume, it was therefore necessary to simulate a large quantity of this isotope in the detector to maximise the amount of  $^{222}\text{Rn}$  events in the region of interest.

The target background activities detailed in Sec. 3.2 were defined so that each background has a similar contribution to that of the  $2\nu\beta\beta$  in the region of



interest [10]. We remind these nominal activities in Tab. 6.2, and give a comparison with the measured activities of the demonstrator source foils contaminations, as well as a calculated limit for the  $^{222}\text{Rn}$  activity inside the tracker volume.

	Nominal activities	Real activities
$^{208}\text{Tl}$	$10 \mu\text{Bq.kg}^{-1}$	$54 \mu\text{Bq.kg}^{-1}$
$^{214}\text{Bi}$	$2 \mu\text{Bq.kg}^{-1}$	$< 290 \mu\text{Bq.kg}^{-1}$
$^{222}\text{Rn}$	$0.15 \text{ mBq.m}^{-3}$	$0.15 \pm 0.02 \text{ mBq.m}^{-3}$ [11]

Table 6.2: Real and targeted nominal activities for the SuperNEMO detector.

### Outside detector backgrounds

This background category is due to the external  $\gamma$ -ray flux produced by radioactive isotope decays in detector components or surrounding laboratory rocks, as well as neutron interactions in the shield and of the detector's material. The limit on external background number of counts set by the NEMO-3 experiment was  $< 0.2$  in the  $2e$  total energy range  $[2.8 - 3.2]$  MeV, for an exposure of  $34.3 \text{ kg.y}$  [12]. Thus, we consider all external backgrounds from outside the foil, apart from  $^{222}\text{Rn}$  in the tracking volume, are expected to be negligible and were not simulated.

We select only events matching the  $2e$  topology. As a reminder, a reconstructed particle is tagged as an electron if it has a negatively curved track with a vertex on the source foils and an associated calorimeter hit. In the following we present an optimisation of the event selection and of the region of interest.

- Justifier bdf externe avec article nemo3 (plus diff roi et meilleure eff)
- Demie vie  $2\nu$  à justifier
- The dominant two neutrino  $2\nu\beta\beta$  background and the background due to foil contaminations were normalised assuming a demonstrator exposure of  $17.5 \text{ kg.y}$ .

## 6.2 Optimisation of event selection

Most of the double beta experiments are only sensitive to the total electron energy sum. Such a variable is presented in Fig. 6.1 in logarithmic scale, for each simulated process detailed in Sec. 6.1. These energy spectra are not normalised, therefore the total number of events for each decay represent the amount of selected  $2e$  topologies. The  $0\nu\beta\beta$  spectrum is peaked around 2.8 MeV, the  $Q_{\beta\beta} = 2.99 \text{ MeV}$  energy being degraded by electron energy losses, explaining the asymmetric energy distribution.

Tab. 6.3 sums up the expected number of counts in the full energy range as well as in the region of interest.

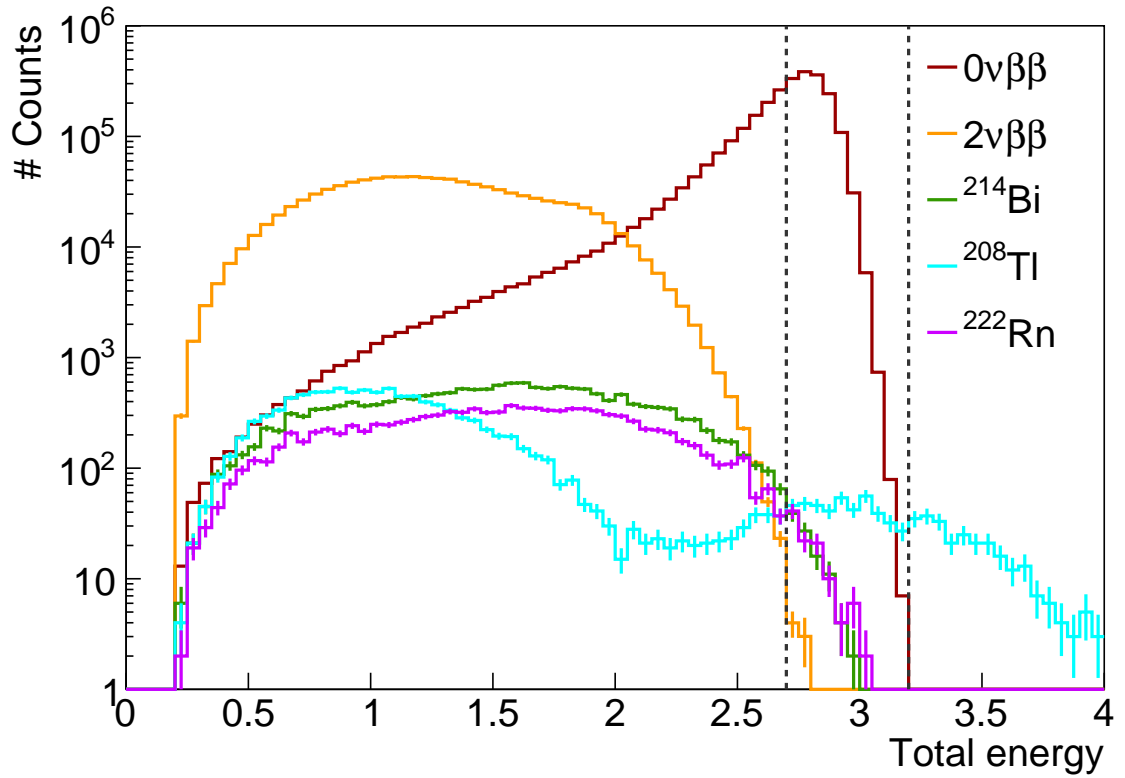


Figure 6.1: Energy spectra for the  $0\nu\beta\beta$  signal and for the main backgrounds. The region of interest is materialised by two dashed vertical lines.  $^{208}\text{Tl}$  events dominate in the ROI.

	Full energy range	[2.75;2.85] MeV
$0\nu\beta\beta$	$2.7 \cdot 10^6$	$9.5 \cdot 10^{-2}$
$2\nu\beta\beta$	$9.1 \cdot 10^5$	$1.1 \cdot 10^{-1}$
$^{208}\text{Tl}$	$1.7 \cdot 10^4$	$9.9 \cdot 10^{-3}$
$^{214}\text{Bi}$	$1.1 \cdot 10^4$	$2.7 \cdot 10^{-2}$
$^{222}\text{Rn}$	$1.1 \cdot 10^4$	

Table 6.3: Real and targeted nominal activities for the SuperNEMO detector.

- plot  $S/\sqrt{B}$  en fonction  $E_i E_{\min}$
- Quel est le signal qu'on cherche
- présentation des cuts
- efficacité des cuts/ signal + bkg
- cuts premier et second ordre

## 6.3 Expected number of background events

- plot energy tot
- plus dans région intérêt

## 6.4 Demonstrator sensitivity

- Résultats  $B = 0$ , avec activités nominales, puis avec activités caca
- Efficiency spretra
- Energy spectra
- Influence des quantités de contaminations sur la sensibilité

### 6.4.1 avec B

Parler du champ non uniforme/attenuation ROI optimization: avec variation coupure énergie

### 6.4.2 sans B

avec variation coupure énergie

### 6.4.3 Champ mappé

## 6.5 HyperNEMO

results for 500kg.y exposure

## 6.6 Other isotopes

distribution  $t_{1/2}$  avec différents échantillons de simus (17.5 kg.y)

## 6.7 Conclusion

- Etude plus générale avec bkg externe+lab (reprendre chiffres NEMO3) + neutrons (cf NEMO3)
- Plot général récap tous résultats



---

## Bibliography

- [1] M. et al. Agostini. Probing majorana neutrinos with double- $\beta$  decay. *Science* 365, 1445, 2019.
- [2] S.I. et al Alvis. Search for neutrinoless double-beta decay in  $^{76}\text{Ge}$  with 26 kg-yr of exposure from the majorana demonstrator. *Phys. Rev. C*, 100, 2019.
- [3] O. et al. Azzolini. First result on the neutrinoless double- $\beta$  decay of  $^{82}\text{Se}$  with cupid-0. *Phys. Rev. Lett.*, 120:232502, Jun 2018.
- [4] C. et al. Alduino. First results from cuore: A search for lepton number violation via  $0\nu\beta\beta$  decay of  $^{130}\text{Te}$ . *Phys. Rev. Lett.*, 120:132501, Mar 2018.
- [5] J. B. et al. Albert. Search for neutrinoless double-beta decay with the upgraded exo-200 detector. *Phys. Rev. Lett.*, 120:072701, Feb 2018.
- [6] A. et al. Gando. Search for majorana neutrinos near the inverted mass hierarchy region with kamland-zen. *Phys. Rev. Lett.*, 117:082503, Aug 2016.
- [7] R. et al. Arnold. Probing new physics models of neutrinoless double beta decay with supernemo. *Eur. Phys. J. C*, 2010.
- [8] S. Clavez. *Development of reconstruction tools and sensitivity of the SuperNEMO demonstrator*. PhD thesis, Université Paris Sud, 2017.
- [9] Tretyak V.I. Ponkratenko O.A. and Zdesenko Yu.G. The event generator decay4 for simulation of doublebeta processes and decay of radioactive nuclei. *Phys. At. Nucl.*, 63:1282–1287, Jul 2000.
- [10] Gomez-Cadenas et al. Physics case of supernemo with  $^{82}\text{Se}$  source. Internal presentation, 2008.
- [11] Xin Ran Liu. Radon mitigation strategy and results for the supernemo experiment. IoP APP / HEPP Conference, 2018.
- [12] R. et al. Arnold. Results of the search for neutrinoless double- $\beta$  decay in  $^{100}\text{Mo}$  with the nemo-3 experiment. *Phys. Rev. D*, 2015.
- [13] Nucleid database.